Electrode-electrolyte interactions on oxide surfaces: the crucial role of surface redox chemistry

Rik V. Mom

r.v.mom@lic.leidenuniv.nl

Leiden University   https://orcid.org/0000-0002-5111-5591

Nipon Deka

Leiden University

Denis Bernsmeier

TU Berlin

Travis Jones

Los Alamos National Laboratory   https://orcid.org/0000-0001-8921-7641

Erdem Irtem

VSParticle BV

Hanna Trzesniowski

Helmholtz Zentrum Berlin

Sheena Louisia

Leiden University

Kees E. Kolmeier

Leiden Institute of Chemistry

Mihaela Gorgoi

Helmholz Zentrum für Materialien und Energie

Patrick Zeller

Fritz Haber Institute of the Max Planck Society

Additional Declarations: There is **NO** Competing Interest.

Abstract

The electric double layer (EDL) formed by ions at the electrode-electrolyte interface is a fundamental component of any electrochemical system, ranging from batteries to fuel cells and electrolyzers[1]. At the atomic level, the behavior of the EDL varies greatly with the choice of electrode, electrolyte, and conditions[2,3]. However, it is thought to follow one general rule analogous to a capacitor[4,5]: low electrode potentials lead to a negative electrode surface charge which attracts cations to the EDL, whereas high potentials lead to a positive surface charge and anion attraction. Here, we show that this most basic rule does not apply for the oxide-electrolyte interface. Using an interface-sensitive X-ray absorption spectroscopy (XAS) approach, we show that increasing the electrode potential attracts cations and repels anions at the IrO_2-electrolyte interface. We show that this behavior is driven by the surface redox chemistry of the oxide, which dictates the surface charge of the electrode by modulating the surface electrophilicity. Our findings rationalize the cation-dependent performance trends observed for oxide electrodes[6−9], paving the way to exploit them in electrolyte engineering.

Main text

When a potential is applied to an electrode, this induces a surface charge, which in turn causes a re-arrangement of the ions and water molecules in the near-surface electrolyte[10]. This dynamic interfacial electrolyte structure, the EDL, is part of the reaction environment at the electrode surface and therefore has marked effect on the kinetics of electrochemical reactions. Exploiting this electrolyte effect to optimize the performance of electrocatalytic devices is challenging, however, because the relationship between the parameters that are controlled, such as the electrolyte pH and cation[11−13]/anion[14−16] composition, and the formed EDL structure is not well understood. This is particularly true for metal oxide electrodes, as here not only the interfacial electrolyte structure is highly dependent on the applied conditions, but also the surface structure of the electrode itself[17−19]. In this study, we set out to determine the impact of this dynamic surface structure on the ion-water-electrode interactions and the resulting EDL structure.

To gain direct insights into the ion-water-electrode interactions at the metal oxide-electrolyte interface, we have designed an interface-sensitive electrochemical X-ray absorption spectroscopy (EC-XAS) approach (figure 1a). Sensitivity to the electrode-electrolyte interface is created by making use of: 1) a mesoporous IrO_2 electrode with an extremely high electrode-electrolyte interface area (figure 1b and section 1 in the SI) and, 2) soft-tender XAS with a probing depth smaller than the electrode thickness. In this way, only the electrolyte inside the pores is probed, which is in large part in contact with the electrode. This allows us to selectively investigate the behavior of interfacial ions through their K-edge XAS spectra. We employed this methodology to examine the interactions of Na^+ and ClO_4^- ions with the IrO_2 electrode in both acidic and alkaline electrolyte, and link this to the observed catalytic activity during the oxygen evolution reaction (OER).

The differences in the OER activity of iridium oxide in acidic and alkaline electrolytes provide a first indication for ion-electrode interactions. Alkaline electrolytes lead to a lower OER activity (figure 1c). Furthermore, the activity in alkaline media depends on the choice of alkali metal cation (figure 1d). These observations suggest that the cations of the electrolyte interact with the OER intermediates under alkaline conditions, thereby affecting the catalytic activity. On the other hand, no cation dependent activity is observed in acidic electrolytes (figure 1e), thus showing the crucial role of the pH in the cation-IrO_2 interactions. These trends are in line with the literature[6,20,21].

In order to examine more closely how Na^+ ions behave in the vicinity of an electrified IrO_2 surface, we stepwise polarized our porous IrO_2 electrode in 0.1M NaOH (pH~13) and 0.1 M $HClO_4$ + 0.1 M $NaClO_4$ (pH~1) and recorded Na K-edge X-ray absorption spectra at every potential step. Since these soft XAS measurements only probe the electrolyte inside the pores, the absolute intensity of the Na K-edge allows us to track the concentration of the sodium ions inside the porous electrode. At pH 1, the Na K-edge spectrum exhibits only a weak signal, and there is no significant change in intensity when varying the potential (figure 2a). These findings indicate that at pH 1, the Na^+ ions are not part of the interfacial electrolyte, in line with the absence of a cation dependent OER activity as shown in figure 1e.

In alkaline electrolyte, Na^+ ions are strongly attracted to the IrO_2 electrode, as seen from the high intensity of the Na K-edge spectra (figure 2b). Furthermore, it can be observed that the cation-IrO_2 interaction is potential-dependent. Based on the concept of capacitive charging[22−26], the traditional view is that when the electrode potential is increased in the positive direction, positively charged cations will be repelled. However, the intensity of the Na K-edge increases when increasing the applied potential. This implies that with the increase in positive potential, more cations are attracted towards the surface. This result shows that the IrO_2-electrolyte interface does not function as a classical capacitor, indicating that interfacial chemistry beyond basic electrostatics plays an important role in the electrode-electrolyte interactions for oxide electrodes.

To obtain a more quantitative view on the Na^+ ions interacting with the IrO_2 surface in 0.1 M NaOH, we combined the XAS data and BET surface area analysis to calculate the approximate Na^+ coverage on the electrode. First, we calculated the Na^+ ion concentration in the porous volume of the catalyst (figure 2c, left axis), utilizing the edge jump intensity of the Na K-edge spectra (calculation in section 5 of SI). We see that the Na^+ ion concentration surges to 3 times the bulk concentration at around 1.0 V_{RHE} and continues to rise at the onset of OER. By incorporating the BET surface area into our calculations, we determined the Na^+ coverage on the electrode (figure 2c right axis, calculation in section 5.4 of SI). At 1.4 V_{RHE} the ion coverage reaches 0.8 Na^+ ion per nm^2. Comparing this to the area occupied by a hydrated Na^+ ion (0.2 nm^2)[27], it is clear that a significant fraction of the surface is covered. This high cation coverage near the electrode surface can be linked to the lower OER activity of IrO_2 in alkaline electrolytes: interfacial ions have been proposed to modify electrocatalytic activity through site blocking,

interactions with reaction intermediates, and alteration of the interfacial water structure (water transport/pH buffering effect)[8,11,28].

To verify our conclusions from the XAS analysis, and extend them to other cations, we tracked the mass of the mesoporous electrode in situ using electrochemical quartz crystal microbalance (EQCM). When cations are attracted to the catalyst, they enter the pores and thereby contribute to the observed mass of the electrode. Such a mass increase equates to a decrease in the quartz crystal resonance frequency. In line with the XAS analysis, figure 2d shows a decrease in resonance frequency with increasingly positive potential, confirming that cations are attracted at more positive potentials. The decrease in oscillation frequency (increase in mass) is larger for heavier cations (K^+, Cs^+) indicating a response based on the choice of cation. Notably, the mass change exhibits two distinct regimes, the first up to 0.6 V_{RHE} and the second from 0.6-1.2V_{RHE} where the latter displays a higher slope. This shows that the cation attraction accelerates at higher potentials, as also confirmed by tracking of the Na K-edge XAS intensity as a function of potential (figure S7b in SI).

To probe the nature of the interaction between the cations and the IrO_2 surface in alkaline electrolytes, we analyzed the shape of the normalized Na K-edge spectra (figure 2e). In the porous volume within the catalyst layer, there are two types of Na^+ ions: those which reside very close to the electrode in the electric double layer and those located at a larger distance from the surface, i.e., bulk electrolyte that is not under the direct influence of the electrode surface and its electric field. A Na^+ ion in the bulk electrolyte can be identified by a Na K-edge spectrum with an unequal intensity ratio of the peaks at 1078.2 eV and 1081.5 eV (dark-yellow dotted spectrum in figure 2e). This spectrum represents fully hydrated Na^+ ions[29]. Noticeably, our operando spectra deviate from this bulk spectrum, exhibiting a higher 1078.2 eV to 1081.5 eV peak intensity ratio (blue spectra in figure 2e). This increase in peak intensity ratio of the Na K-edge spectrum is the signature of the distortion and opening of the hydration shell of the Na^+ ion, as shown both experimentally and theoretically[30−32]. This indicates that upon interaction with the IrO_2 surface, the Na^+ ions loose part of their hydration shell. Thus, the Na^+ ions interact directly with the oxide surface and its active OER sites, which will directly impact the stability of the catalytic intermediates.

In figure 2e, it can be noted that the 1078.2 eV/1081.5 eV intensity ratio is potential dependent. In part, this can be explained by an increasing Na^+ concentration in the double layer at more positive potentials, because this increases the contribution of adsorbed Na^+ with respect to Na^+ in the bulk electrolyte. However, if we subtract the bulk contribution using the spectrum recorded at pH 1, which only contains the bulk contribution, there is still a steady rise in the 1078.2 eV/1081.5 eV peak intensity ratio (figure 2f and section 7 in SI). This implies that when the electrode surface becomes increasingly crowded with Na^+ ions at high potentials, the hydration shell of the ions is further distorted. To confirm that these strong hydration shell distortions are the result of Na^+ adsorption rather than Na^+ intercalation into the oxide lattice, we monitored the IrO_2 lattice oxygen peak at 530 eV in the O K-edge. We observed no

changes as a function of time or potential, indicating that the lattice distortion/break-up required for Na^+ intercalation into the rutile lattice did not occur.

In the following, we will show that the observed strong Na^+- IrO_2 interactions and their unexpected potential dependence are intimately linked to the surface chemistry of the IrO_2 electrode. To investigate this surface chemistry, we recorded *operando* O K-edge XAS spectra. The spectral range spanning 527-530 eV in the O K-edge data provides insights into the behavior of surface oxygen atoms in iridium oxide[18]. These surface oxygen atoms fall into three categories: 1) H_2O/OH/O bound to one Ir atom at the CUS (coordinatively unsaturated sites), which we term e.g., μ_1-OH, 2) OH/O bound to two Ir atoms at bridge sites, which we term e.g., μ_2-OH, and 3) O atoms bound to three Ir atoms as in bulk IrO_2, which we label μ_3-O. Since the μ_3-O atoms are inert[18,33], we focus on the μ_1- and μ_2- groups here. These groups strongly differ in their O K-edge spectrum, as shown in previous work[18,33−35]. This can be used to explain the *operando* data in figure 3(a-b). The low intensity in the 527-530 eV window observed at ≤0.35 V_{RHE} in both acidic and alkaline electrolyte is consistent with μ_1-OH_2, μ_1-OH, and μ_2-OH surface groups which display almost no intensity in this potential range. The increasing intensity at 529 eV at higher potentials can be attributed to μ_2-O formation through the deprotonation reaction μ_2-OH à μ_2-O + H^+ + e^- in acid and μ_2-OH + OH^- à μ_2-O + H_2O + e^- in alkaline electrolyte. Above ~1.2 V_{RHE}, a broadening towards lower excitation energies is observed, which is attributed to the formation of μ_1-O through μ_1-OH à μ_1-O + H^+ + e^- in acid and μ_1-OH + OH^- à μ_1-O + H_2O + e^- in alkaline electrolyte. Note that due to acid-base reactions, μ_1-O^- and μ_2-O^- may also be present in alkaline electrolyte, while e.g., μ_2-OH^+ might be formed in acid. This could explain the differences in observed O K-edge spectra in alkaline and acid media. The common denominator, however, is that the surface becomes strongly electrophilic due to the oxidative deprotonation of the surface -OH groups with the increase in potential.

To understand the influence of the deprotonation reaction on the IrO_2 electrode at increasingly positive potential, we computed the charge on the electrode surface through DFT-RISM[36,37] calculations (details in section 9 of SI). Specifically, we compared the surface charge on a partially protonated (reduced) surface to a deprotonated surface (oxidized) in acidic and alkaline environment (figure 3c). For both electrolytes, we see that the oxidized surface possesses higher negative charge compared to the reduced surface. Based on this, we conclude that the electrophilic μ_1-O and μ_2-O groups at the oxidized surface attract electron density towards the surface (figure 3d). This accumulation of negative charge at the surface is compensated by ions from the electrolyte. In alkaline electrolyte, the overall process is:

$$OH_{ads} + n\ Na^+ + OH^- \rightarrow O_{ads} + (1\text{-}n)\ e^- + n\ Na^+_{ads} + H_2O \qquad (1)$$
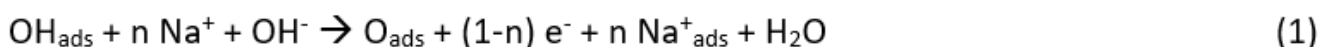
In agreement with the experiments, this leads to an increased interfacial Na^+ concentration in alkaline electrolyte. Furthermore, reaction 1 explains why the cyclic voltammogram of iridium oxides shows a super-Nernstian shift of the surface redox features when increasing the pH[20,38] (see section 8 in SI), because the number of transferred electrons (1-n) is smaller than the number of transferred protons (1).

According to the calculations, the same deprotonation-induced decrease in surface charge should occur in acidic electrolyte. However, no Na^+ attraction is observed in the pH 1 experiments. This can be rationalized by considering the acid-base chemistry of the surface, which is not fully captured in the calculations, but was already hinted at by the O K-edge spectra. Such acid-base reactions may generate Ir-O-H$^+$ groups in acid, leading to a positive surface charge that repels the Na^+ ions and instead attracts ClO_4^- ions. If oxidative deprotonation makes this positively charged surface less positive at elevated potential, this should repel the ClO_4^- ions through the reaction:

$$OH_{ads} + n\ ClO_{4\ ads}^- \rightarrow O_{ads} + (1-n)\ e^- + n\ ClO_4^- + H^+ \tag{2}$$
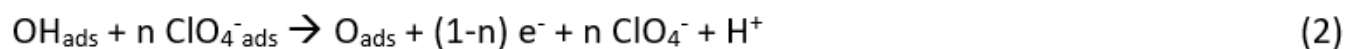
To test this hypothesis, we probed the concentration of perchlorate ions near the IrO_2 surface using Cl K-edge spectra[39,40] and EQCM. Indeed, we see that the Cl K-edge intensity decreases with the increase in applied potential (figure 4a). Similarly, a decrease in mass is observed in EQCM is due to the expulsion of ClO_4^- ions out of the porous electrode at increasingly positive potentials (figure 4b). This confirms our hypothesis and shows the generality of the mechanism uncovered here: whenever the oxide surface is oxidized, this will increase its electrophilicity, drawing negative charge to the surface, attracting or repelling electrolyte ions. Importantly, oxide surface redox is not particular for IrO_2, it is widely observed for oxide materials used in electrochemistry[6,16,41−45]. Furthermore, the driving force for ion adsorption is essentially purely electrostatic (figure S11 in SI) and will therefore occur for any ion. Therefore, we expect that the surface redox effect on ion-oxide interactions is an omnipresent phenomenon in oxide electrochemistry.

Declarations

References

1. Stamenkovic, V. R., Strmcnik, D., Lopes, P. P. & Markovic, N. M. Energy and fuels from electrochemical interfaces. *Nature Materials* vol. 16 (2016).

2. Haid, R. W., Ding, X., Sarpey, T. K., Bandarenka, A. S. & Garlyyev, B. Exploration of the electrical double-layer structure: Influence of electrolyte components on the double-layer capacitance and potential of maximum entropy. *Current Opinion in Electrochemistry* vol. 32 (2022).

3. Sebastián-Pascual, P., Shao-Horn, Y. & Escudero-Escribano, M. Toward understanding the role of the electric double layer structure and electrolyte effects on well-defined interfaces for electrocatalysis. *Current Opinion in Electrochemistry* vol. 32 (2022).

4. Grahame, D. C. The electrical double layer and the theory of electrocapillarity. *Chem. Rev.* **41**, (1947).

5. Damaskin, B. B. & Petrii, O. A. Historical development of theories of the electrochemical double layer. *Journal of Solid State Electrochemistry* vol. 15 (2011).

6. Suntivich, J., Perry, E. E., Gasteiger, H. A. & Shao-Horn, Y. The Influence of the Cation on the Oxygen Reduction and Evolution Activities of Oxide Surfaces in Alkaline Electrolyte. *Electrocatalysis* **4**, (2013).

7. Tymoczko, J., Colic, V., Ganassin, A., Schuhmann, W. & Bandarenka, A. S. Influence of the alkali metal cations on the activity of Pt(1 1 1) towards model electrocatalytic reactions in acidic sulfuric media. *Catal. Today* **244**, (2015).

8. Huang, J., Li, M., Eslamibidgoli, M. J., Eikerling, M. & Groß, A. Cation Overcrowding Effect on the Oxygen Evolution Reaction. *JACS Au* **1**, (2021).

9. Görlin, M. *et al.* Key activity descriptors of nickel-iron oxygen evolution electrocatalysts in the presence of alkali metal cations. *Nat. Commun.* **11**, (2020).

10. Favaro, M. *et al.* Unravelling the electrochemical double layer by direct probing of the solid/liquid interface. *Nat. Commun.* **7**, (2016).

11. Waegele, M. M., Gunathunge, C. M., Li, J. & Li, X. How cations affect the electric double layer and the rates and selectivity of electrocatalytic processes. *J. Chem. Phys.* **151**, (2019).

12. Khani, H., Puente Santiago, A. R. & He, T. An Interfacial View of Cation Effects on Electrocatalysis Systems. *Angewandte Chemie - International Edition* vol. 62 (2023).

13. Qin, X., Hansen, H. A., Honkala, K. & Melander, M. M. Cation-induced changes in the inner- and outer-sphere mechanisms of electrocatalytic CO_2 reduction. *Nat. Commun.* **14**, (2023).

14. Kamat, G. A. *et al.* Acid anion electrolyte effects on platinum for oxygen and hydrogen electrocatalysis. *Commun. Chem.* **5**, (2022).

15. Arminio-Ravelo, J. A., Jensen, A. W., Jensen, K. D., Quinson, J. & Escudero-Escribano, M. Electrolyte Effects on the Electrocatalytic Performance of Iridium-Based Nanoparticles for Oxygen Evolution in Rotating Disc Electrodes. *ChemPhysChem* **20**, (2019).

16. Navodye, S. A. K. & Gunasooriya, G. T. K. K. Acid Electrolyte Anions Adsorption Effects on IrO_2 Electrocatalysts for Oxygen Evolution Reaction. *J. Phys. Chem. C* **128**, 6041–6052 (2024).

17. Deka, N. *et al.* On the Operando Structure of Ruthenium Oxides during the Oxygen Evolution Reaction in Acidic Media. *ACS Catal.* **13**, (2023).

18. Mom, R. V. *et al.* Operando Structure-Activity-Stability Relationship of Iridium Oxides during the Oxygen Evolution Reaction. *ACS Catal.* **12**, 5174–5184 (2022).

19. Görlin, M. *et al.* Oxygen evolution reaction dynamics, faradaic charge efficiency, and the active metal redox states of Ni-Fe oxide water splitting electrocatalysts. *J. Am. Chem. Soc.* **138**, 5603–5614 (2016).

20. Kuo, D. Y. *et al.* Influence of Surface Adsorption on the Oxygen Evolution Reaction on IrO2(110). *J. Am. Chem. Soc.* **139**, (2017).

21. Michael, J. D. *et al.* Alkaline electrolyte and fe impurity effects on the performance and active-phase structure of niooh thin films for OER catalysis applications. *J. Phys. Chem. C* **119**, (2015).

22. Helmholtz, H. Ueber einige Gesetze der Vertheilung elektrischer Ströme in körperlichen Leitern mit Anwendung auf die thierisch-elektrischen Versuche. *Ann. Phys.* **165**, (1853).

23. Gouy, M. Sur la constitution de la charge électrique à la surface d'un électrolyte. *J. Phys. Théorique Appliquée* **9**, (1910).

24. Chapman, D. L. LI. A contribution to the theory of electrocapillarity . *London, Edinburgh, Dublin Philos. Mag. J. Sci.* **25**, (1913).

25. Stern, O. ZUR THEORIE DER ELEKTROLYTISCHEN DOPPELSCHICHT. *Zeitschrift für Elektrochemie und Angew. Phys. Chemie* **30**, (1924).

26. Devanathan, M. A. V. & Tilak, B. V. K. S. R. A. The Structure of the Electrical Double Layer at the Metal-Solution Interface. *Chem. Rev.* **65**, (1965).

27. Mähler, J. & Persson, I. A study of the hydration of the alkali metal ions in aqueous solution. *Inorg. Chem.* **51**, (2012).

28. del Rosario, J. A. D., Li, G., Labata, M. F. M., Ocon, J. D. & Chuang, P. Y. A. Unravelling the roles of alkali-metal cations for the enhanced oxygen evolution reaction in alkaline media. *Appl. Catal. B Environ.* **288**, (2021).

29. Aziz, E. F., Zimina, A., Freiwald, M., Eisebitt, S. & Eberhardt, W. Molecular and electronic structure in NaCl electrolytes of varying concentration: Identification of spectral fingerprints. *J. Chem. Phys.* **124**, (2006).

30. Galib, M. *et al.* Revisiting the hydration structure of aqueous Na+. *J. Chem. Phys.* **146**, (2017).

31. Galib, M., Schenter, G. K., Mundy, C. J., Govind, N. & Fulton, J. L. Unraveling the spectral signatures of solvent ordering in K-edge XANES of aqueous Na+. *J. Chem. Phys.* **149**, (2018).

32. Aziz, E. F., Freiwald, M., Eisebitt, S. & Eberhardt, W. Steric hindrance of ion-ion interaction in electrolytes. *Phys. Rev. B - Condens. Matter Mater. Phys.* **73**, (2006).

33. Frevel, L. J. *et al.* In situ X-ray spectroscopy of the electrochemical development of iridium nanoparticles in confined electrolyte. *J. Phys. Chem. C* **123**, 9146–9152 (2019).

34. Nong, H. N. *et al.* Key role of chemistry versus bias in electrocatalytic oxygen evolution. *Nature* **587**, 408–413 (2020).

35. Pfeifer, V. *et al.* In situ observation of reactive oxygen species forming on oxygen-evolving iridium surfaces. *Chem. Sci.* **8**, 2143–2149 (2017).

36. Nishihara, S. & Otani, M. Hybrid solvation models for bulk, interface, and membrane: Reference interaction site methods coupled with density functional theory. *Phys. Rev. B* **96**, (2017).

37. Schmickler, W. Double layer theory. *J. Solid State Electrochem.* **24**, (2020).

38. Ooka, H., Yamaguchi, A., Takashima, T., Hashimoto, K. & Nakamura, R. Efficiency of Oxygen Evolution on Iridium Oxide Determined from the pH Dependence of Charge Accumulation. *J. Phys. Chem. C* **121**, (2017).

39. Vaudey, C. E. *et al.* Chlorine speciation in nuclear graphite studied by X-ray Absorption Near Edge Structure. *J. Nucl. Mater.* **418**, (2011).

40. Nakanishi, K. & Ohta, T. Verification of the FEFF simulations to K-edge XANES spectra of the third row elements. *J. Phys. Condens. Matter* **21**, (2009).

41. Strmcnik, D. *et al.* The role of non-covalent interactions in electrocatalytic fuel-cell reactions on platinum. *Nat. Chem.* **1**, (2009).

42. Stoerzinger, K. A. *et al.* The Role of Ru Redox in pH-Dependent Oxygen Evolution on Rutile Ruthenium Dioxide Surfaces. *Chem* **2**, (2017).

43. Giordano, L. *et al.* PH dependence of OER activity of oxides: Current and future perspectives. *Catalysis Today* vol. 262 (2016).

44. Knijff, L., Jia, M. & Zhang, C. Electric double layer at the metal-oxide/electrolyte interface. in *Encyclopedia of Solid-Liquid Interfaces* vols 1–3 (2023).

45. Jia, M., Zhang, C. & Cheng, J. Origin of Asymmetric Electric Double Layers at Electrified Oxide/Electrolyte Interfaces. *J. Phys. Chem. Lett.* **12**, (2021).
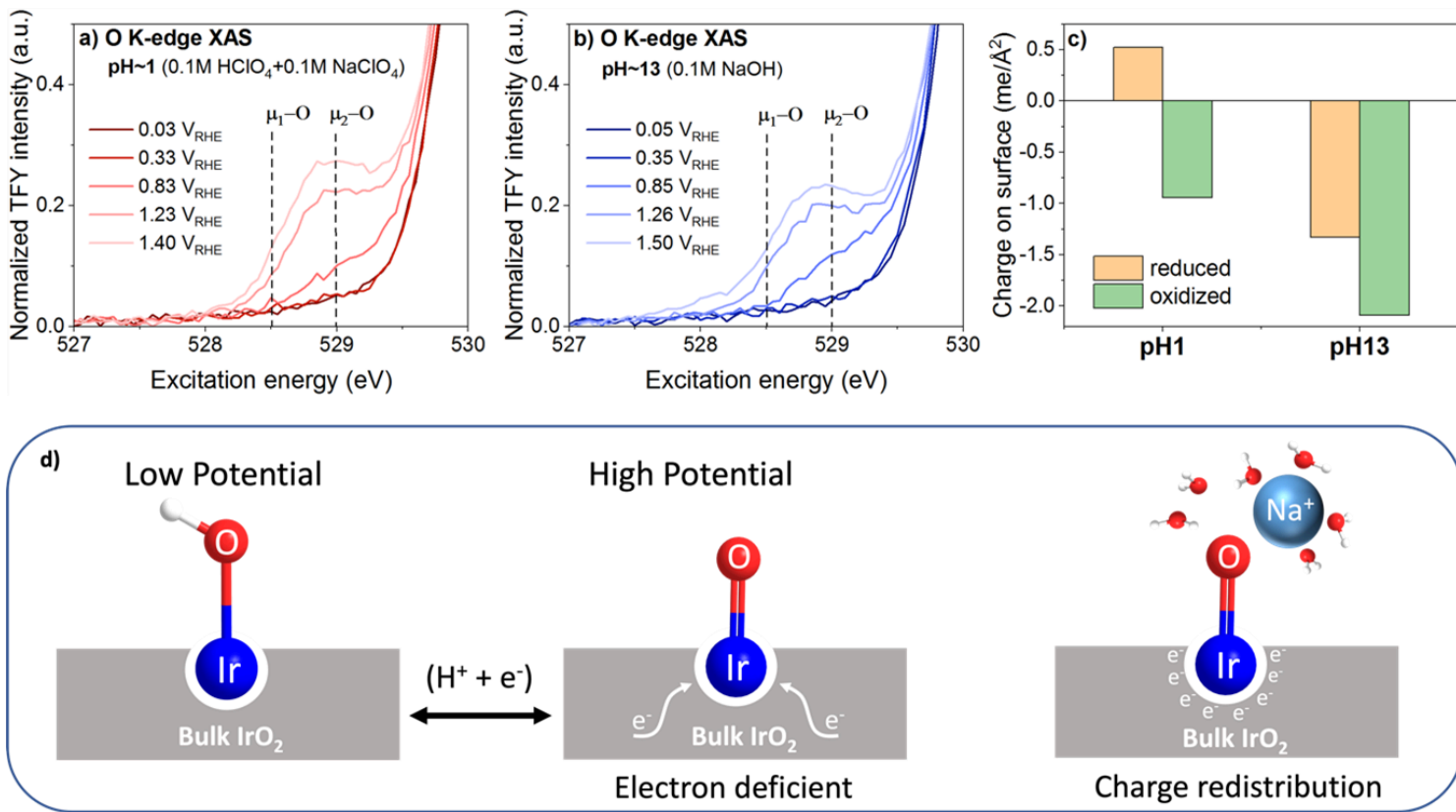
Figures
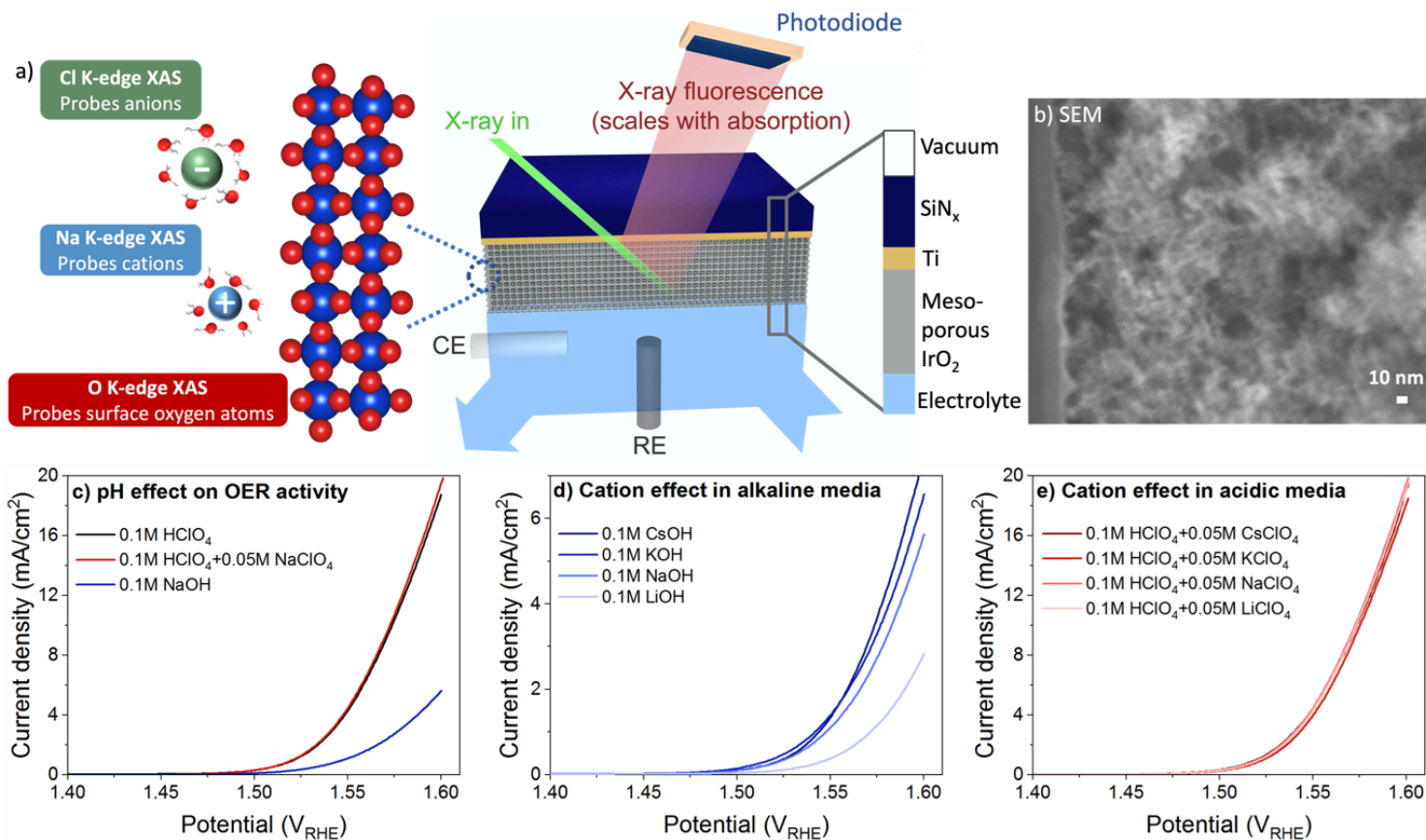
Figure 1

a) Schematic of the experiment (blue and red spheres represent the iridium and oxygen atoms respectively), b) cross-section SEM micrograph of the mesoporous IrO_2 film, c-e) effect of pH, cations in alkaline, and acidic electrolytes on OER activity of IrO_2 respectively.
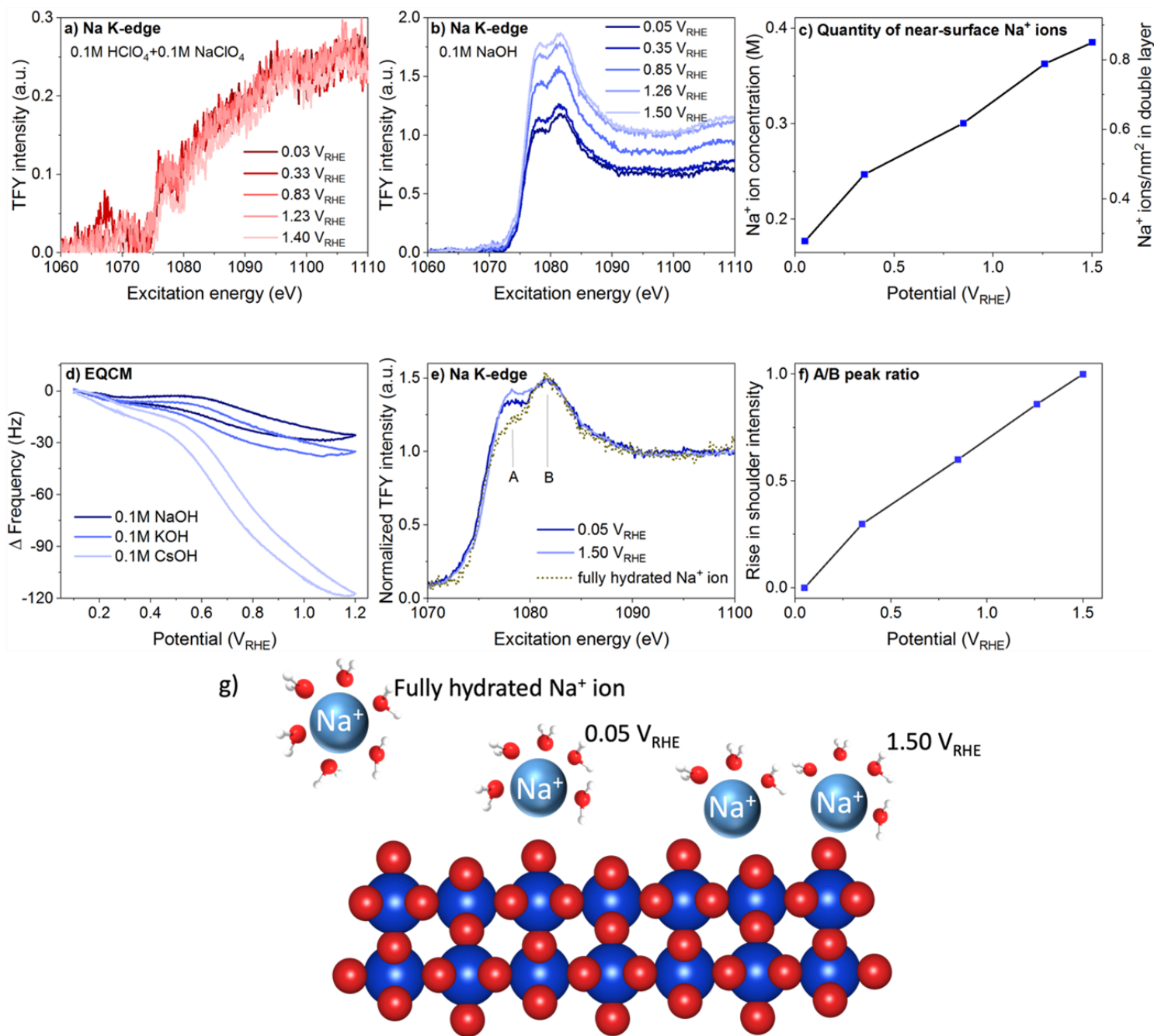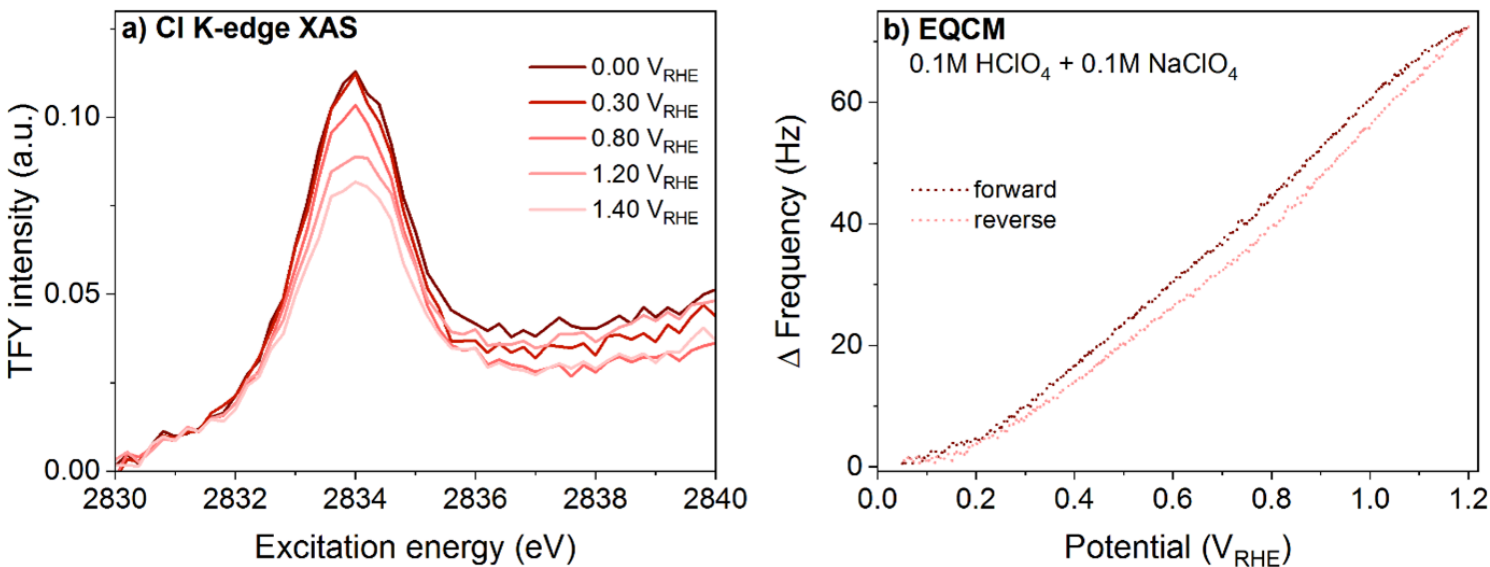
Figure 2

a-b) Operando Na K-edge absorption spectra of Na$^+$ near an IrO$_2$ surface at pH~1 (0.1M HClO$_4$+0.1M NaClO$_4$) and pH~13 (0.1M NaOH). c) Calculated concentration of Na$^+$ in the pores and the number of Na$^+$ per unit area of the double layer. d) frequency response of an IrO$_2$ coated quartz crystal in alkaline electrolytes, e) Normalized Na K-edge spectra of Na$^+$ near IrO$_2$ surface at pH~13 (0.1M NaOH) f) Variation of shoulder (1078.2 eV) to white line (1081.5 eV) intensity ratio with applied potential, g) ball model showing Na$^+$ adsorption at high potential.

Figure 3

a-b) Operando O K-edge spectra of IrO$_2$ at pH~1 (0.1M HClO$_4$+0.1M NaClO$_4$) and pH~13 (0.1M NaOH) respectively. Both spectra are normalized to the edge jump at 550 eV, c) theoretically calculated charge on the surface at 1.5 V$_{RHE}$, d) Proposed mechanism for oxidation-induced surface charging.

Figure 4

a) Cl K-edge XAS of ClO$_4^-$ ions near IrO$_2$ surface, b) EQCM in 0.1M HClO$_4$+0.1M NaClO$_4$.

Supplementary Files

This is a list of supplementary files associated with this preprint. Click to download.

- SIProbingnearsurfaceionsiniridiumoxideV10.docx